AFM and TEM image of phenylacetylene polymerization on Rh/PVP colloidal nanoparticles

Marta Kopaczyńska,[a] Jurgen H. Fuhrhop,[a] Anna M. Trzeciak,*[b] Józef J. Ziółkowski[b] and Robert Choukroun[c]

Received (in Durham, UK) 18th January 2008, Accepted 13th March 2008
First published as an Advance Article on the web 28th April 2008
DOI: 10.1039/b800867a

Rh/PVP nanoparticles were used as a new kind of catalyst in polymerization of phenylacetylene (PA). Polyphenylacetylene (PPA), purely *cis*-transoidal, was obtained with a yield up to 90% and molecular weights equal from 21 100 to 140 700. The polymerization reaction was monitored by AFM (atomic force microscopy) and TEM (transmission electron microscopy) methods. Before polymerization, spontaneous aggregation of Rh/PVP nanoparticles in methanol into dense spherical nanostructures having a tendency to form ordered superstructures upon drying, was observed. The formation and increase of PPA fibres around Rh nanoparticles was followed in time with AFM and TEM. The stretched PPA fibres adopt a helical structure with a pitch of about 5 nm.

Introduction

There are many examples of the successful application of transition metal nanoparticles as catalysts in hydrogenation of hydrocarbons[1] and the C–C cross-coupling,[2] as well as in the carbonylation of aryl halides.[3] The water soluble PVP (polyvinylpyrrolidone) polymer acted in all cases as a steric stabilizer of nanoparticles by diminishing the van der Waals interactions, that cause coagulation of the particles.[4,5]

Rhodium nanoparticles stabilized by polyvinylpyrrolidone, Rh/PVP, exhibited in particular a high catalytic activity in the hydrogenation of benzene and phenylacetylene.[6] The best results were obtained when the reaction was performed in a heterogeneous system, without solvent, as well as in a biphasic water–benzene system. However, when methanol was used as a reaction medium, benzene was not hydrogenated.[6]

In this paper, we present for the first time studies of PA polymerization on the surface of Rh/PVP colloidal nanoparticles.

Typical Rh-catalyst used in phenylacetylene polymerization presents a Rh(I) complex with a cyclooctadiene (cod) or norbornadiene (nbd) ligand in a coordination sphere.[7] In fact, there are no examples of active catalyst precursors containing Rh(0) species. The catalytic system based on Rh/PVP is unique for two reasons: first, it is active in the absence of dienes (cod or nbd) and second, it produces polyphenylacetylene (PPA) with a reasonable high yield in heterogeneous (solvent free) as well as in homogeneous systems (Table 1).

Application of the atomic force microscopy (AFM) method in our system allowed the observation of the polymerization process in time and to collect the unique pictures of both Rh/PVP nanoparticles and of helical PPA chains formed during the polymerization reaction. Until now, very few attempts have been made to observe synthetic helical polymers using AFM and STM techniques.[8,9]

Experimental

Reagents

Rh/PVP was obtained according to the literature method.[10]

Phenylacetylene (PA) was acquired from Aldrich. Analytical-grade methanol and chloroform were purchased from POCh (Gliwice, Poland).

Tapping mode AFM measurements

The initial stages of phenylacetylene polymerization catalyzed by Rh/PVP colloid were imaged by AFM using a MultiMode IIIa scanning probe microscope with extender module (Digital Instruments, Inc., Santa Barbara, CA, USA) in the dynamical modus. An active vibration isolation platform, Halyonics, Mod. 1, was applied and height measurements with an

Table 1 Results of PA polymerization with (Rh-PVP) catalyst

Solvent	Co-catalyst	Yield of PPA (%)	M_w
—	—	25	42 300
—	1,5-cod	65	21 000
MeOH	1,5-cod	65	67 600
MeOH	Cyclooctene	33	100 000
$CHCl_3$	1,5-cod	10	10 100
CH_3OH + $CHCl_3$	—	47	108 500
CH_3OH + $CHCl_3$	1,5-cod	70	30 100
CH_3OH + $CHCl_3$	1,3-cod	80	65 400
CH_3OH + $CHCl_3$	1,3-Cyclohexadiene	30	140 700
CH_3OH + $CHCl_3$	1,4-Cyclohexadiene	20	138 000
CH_3OH + $CHCl_3$	Cyclooctene	90	75 000

Reaction conditions: [PhC≡CH] : [Rh] = 370; [PhC≡CH] = 1.86×10^{-3} mol; [Rh] = 5×10^{-6} mol; [co-catalyst] = 1–3 × 10^{-4} mol; $V_{solvent}$ 0.6 mL; 17 h, room temp.

[a] *Freie Universität Berlin, FB Biologie, Chemie, Pharmazie, Institut für Organische Chemie Taku Str. 3, D-14195 Berlin, Germany*
[b] *Department of Chemistry, University of Wroclaw, 14 F. Joliot-Curie Str., 50-383 Wroclaw, Poland*
[c] *Laboratoire de Chimie de Coordination du CNRS (UPR 8241), 205 route de Narbonne, 31077 Toulouse cedex 4, France*

instrumental, vertical resolution of ±0.2 nm were usually performed at night. The silicon cantilevers were used with a typical resonance frequency in the range of 200–400 kHz and a spring constant of 48 N m^{-1}.

The scan angle was maintained at 0, and the images were captured in the trace direction with a scan rate from 0.500 to 1.500 Hz. All samples were measured at room temperature in air environment. The sample was first adjusted with an optical light microscope (Nanoscope, Optical Viewing System).

Height-resolution-images were obtained with a Super Sharp Silicon cantilever with a typical tip radius of 2 nm, at a low-frequency F_0 = 80–200 kHz and a force constant 5–37 N m^{-1}. The set-point amplitude of the cantilever was maintained by the feedback circuitry to 80% of the free oscillation amplitude of the cantilever.

Height and width measurements from AFM images were made with Digital Instruments Nanoscope Software version 5.12r2. Data-analysis was performed after plane-fit, height measurements based on the cross-sectional profiles.

Since section analysis is typically used to evaluate height and width in AFM images, a quantitative study was undertaken to test agreement in measurements made using bearing analysis *versus* those made using section analysis.

Preparation of samples for AFM measurements

10 μL of colloidal solution containing 0.01343 g of Rh/PVP (1.28×10^{-5} mol Rh) and PA in a ratio [PA] : [Rh] 50 : 1 or 5 : 1 in methanol (0.013 mL) was placed onto the freshly cleaved mica platelet and the excess fluid was blotted off after 15 s and then dried in a nitrogen stream. For imaging of polymer fibres formed during polymerization process, the spin-coating method was used with the speed 4000 rpm, 2 min. Spin-coating is a very convenient procedure to stretch molecules and fibres like polymers on the surface.

TEM measurements

Observation of the PA polymerization reaction catalyzed by Rh/PVP colloids and the detection of PPA were imaged using a Philips CM12 transmission electron microscope operated at 100 kV. Transmission electron microscopy (TEM) samples were prepared by dropping 5 μL of a colloidal solution of Rh/PVP onto a carbon grid. After 1 min, the remaining solution was blotted off with filter paper without staining solution in the case of imaging Rh nanoparticles or with 1% phosphotungstate acid (PTA) in the case of imaging PPA polymers.

Polymerization reaction procedure

Polymerization reactions were carried out in 50 mL Schlenk flasks under a nitrogen atmosphere. In a typical experiment, a sample of Rh/PVP colloid containing 5×10^{-6} mol of rhodium was dissolved in 0.6 mL of $CHCl_3$ + CH_3OH (1 : 1) mixture and 0.2 mL (1.86 mmol) of PA was added. The mixture was stirred under nitrogen at 25 °C for 17 h, then the polymer was precipitated by the addition of methanol (2 mL), filtered off, and dried in vacuum.

Polymer yields were determined by weight. Molecular weight of PPA was determined by a HPLC method (Hewlett-Packard) using polystyrene samples of known M_w for standardisation.

The stereostructure of the PPA was determined as 100% *cis*-transoidal according to literature methods based on ^{1}H NMR and IR data.[11,12]

Results and discussion

Polymerization of phenylacetylene catalyzed by Rh/PVP colloid

The first tests show that Rh/PVP catalysed polymerization of phenylacetylene at room temperature produced 25% of PPA (M_w 42 300) after 17 h in the absence of any solvent. Addition of 1,5-cod in *ca.* 100-fold excess in respect to rhodium caused an increase of the polymerization reaction yield but the M_w value decreased to 21 000. In further experiments performed in methanol as a solvent, polymerization occurred smoothly with an increase of M_w up to 67 600. However, in $CHCl_3$ in which Rh/PVP colloid is not dissolved, only 10% of PPA was obtained.

The 1 : 1 mixture of $CHCl_3$: CH_3OH was experimentally found as the best one for the performance of catalytic reactions. In the absence of any co-catalyst, with only Rh/PVP, 47% of PPA (M_w 108 500) was obtained. The effect of olefins added as co-catalysts is demonstrated in Table 1. It is clearly seen that unsaturated co-catalysts, like cod, cyclooctene or cyclohexadienes, are modifying the catalytic activity of Rh/PVP. Interaction of Rh/PVP with 1,3-cyclohexadiene and 1,4-cyclohexadiene seems to be quite strong and leads to the significant decrease of PPA yield. However, in the same time M_w reached the highest values 138 000–140 700 (Table 1). In all the reactions with the Rh/PVP catalyst, only one *cis*-transoidal isomer of PPA was formed. Surprisingly, there is no clear correlation between the kind of co-catalyst used and polydispersion (M_w/M_n) of the PPA. In a series of experiments performed in CH_3OH + $CHCl_3$, the polydispersion ranged from 2.1 to 2.5.

Formation of Rh/PVP aggregates in methanol

The main characteristic feature of the Rh/PVP colloids investigated in this paper is the small size of the Rh nanoparticles, 4–5 nm in diameter (Fig. 1a and b). However, in the presence of methanol the intensive aggregation was observed using AFM and TEM methods. To confirm that the nanoparticle aggregates are spherical and not flat we analyzed their heights. The spherical aggregates, which generally have diameters between 10–100 nm are built from smaller 4–5 nm Rh particles (Fig. 1c).

From this finding one may conclude, that the aggregation in methanol should not be detrimental to the catalytic activity of the nanoparticles, since their active surface remains more or less unchanged.

AFM studies of PPA formation

To study the polymerization process by AFM, a spin-coating method was used. The Rh/PVP colloid dissolved in methanol was mixed with PA at the ratio [PA] : [Rh] = 5 : 1 and immediately fixed on mica platelets by spin-coating.

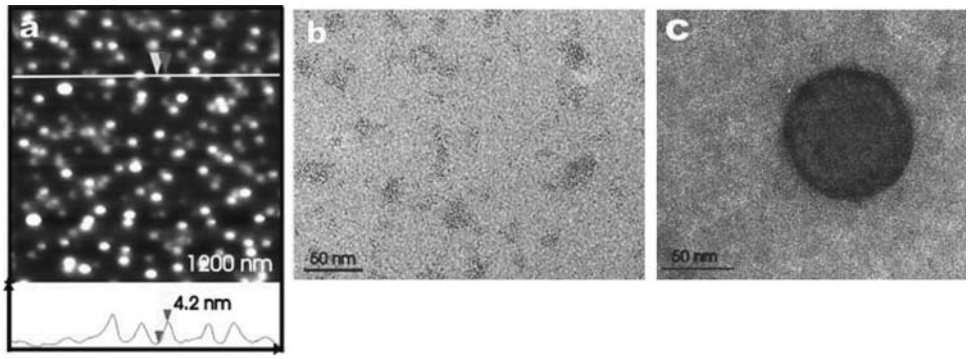

Fig. 1 Images of Rh nanoparticles stabilized by PVP on mica surface. (a) AFM image with height diagram; TEM images of (b) Rh nanoparticles deposited on carbon grid, (c) a spherical agglomerate from methanol solution.

The time dependent formation of PPA around the rhodium nanoparticles was directly observed by AFM after 30 min (Fig. 2) and after 24 h (Fig. 3). After 30 min a layer of the PPA polymer, up to 20 nm, formed around each catalytically active particle was observed.

TEM images showed ordered crystallites of PPA fibres with diameters between 0.8 and 1.0 nm (Fig. 3a), which agrees nicely with the diameter of the PPA-chain. The 4–5 nm Rh nanoparticles were invisible in the huge concentration of the PPA polymers.

After 24 h a large number of long and cross-linked polymer fibres on the mica surface was seen in AFM images. Rh nanoparticles were no more visible because of the large amount of PPA polymer (Fig. 3b).

The visualization of the individual PPA polymer fiber on the surface was achieved by overstretching with a flat stream of nitrogen gas or by application of spin-coating directly on mica from very dilute solutions where 4–5 nm of Rh particles were also imaged next to the PPA fibres (Fig. 4a). To the best of our knowledge it is the first detection of spectacular helical PPA polymer by high-resolution AFM images (Fig. 4b and c).

The height of the separately stretched polymer chain was determined to be 1.0 nm ± 0.2 nm from the cross-section profile and the length of the singular polymer ranged from 100 nm up to 5 μm. Observable *cis*-transoidal PPA adopt a helical shape with a pitch of about 5 nm (Fig. 4c). The distance between the individual turns of the screw is thus exceedingly small and at the limits of vertical resolution of AFM measurements for the commercial tips that were used. A "super sharp" 2 nm silicon tip was applied at an extremely low set point

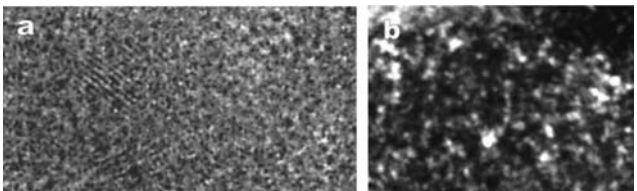

Fig. 3 (a) TEM image of the crystallite on carbon grid, (b) AFM image of the PPA polymers 24 h after reaction.

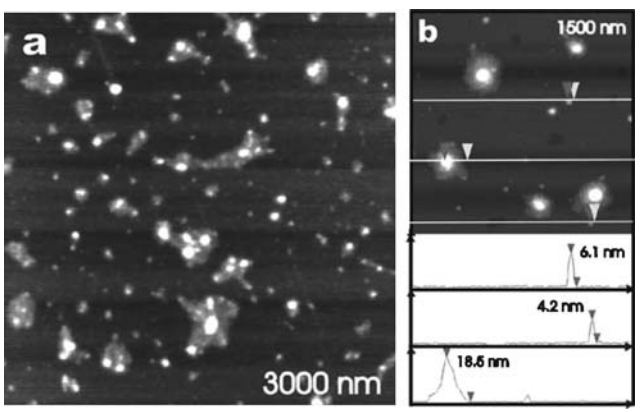

Fig. 2 AFM images of PPA covering on the Rh nanoparticles after 30 min.

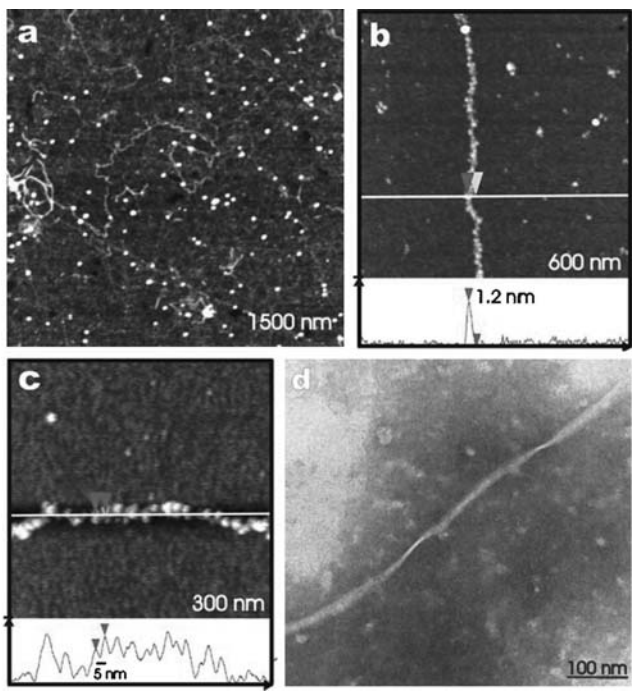

Fig. 4 (a), (b), (c) AFM images of stretched PPA polymers on mica surface, (d) TEM measurements of the PPA polymers on carbon grid.

amplitude typical for application on soft materials, and the measurements were repeated several times to guarantee reproducibility. However, the geometry of the triangular tip caused broadening effects and difficulties in measurements of the pitch in the helical structures. These effects do not allow the suggestion of a correct model for helical PPA with a pitch measured in AFM. We may solve that problem in the future by using carbon nanotube tips with the tip radius below 2 nm.

TEM images of PPA polymers fully confirmed the diameter and helicity of the singular polymer: single fibres have a diameter of about one nanometre, thicker fibres with diameter up to 20 nm and lengths of few micrometres are aggregates of the 1 nm strands (Fig. 4d).

Conclusions

In this paper we demonstrated for the first time the catalytic activity of Rh/PVP colloids in the polymerization of phenylacetylene. The polymerization reaction was monitored *in situ* by AFM and TEM methods and formation of PPA fibres around Rh nanoparticles was shown. The helical structure of PPA was confirmed by analysis of separately stretched polymer chains.

Acknowledgements

This research was supported by the Polish Ministry of Science and Higher Education through the project PBZ-KBN-116/T09/2004. The financial support is gratefully acknowledged.

References

1 J. D. Aiken III and G. R. Finke, *J. Mol. Catal. A: Chem.*, 1999, **145**, 1.
2 J. G. de Vries, *Dalton Trans.*, 2006, 421–429.
3 W. Wojtków, A. M. Trzeciak, R. Choukroun and J.-L. Pellegatta, *J. Mol. Catal. A: Chem.*, 2004, **224**, 81.
4 S. K. Shaikhutdinov and F. J. Cadete Santos Aires, *Langmuir*, 1998, **14**, 3501–3505.
5 T. D. Ewers, A. K. Sra, B. C. Norris, R. E. Cable, C.-H. Cheng, D. F. Shantz and R. E. Shaak, *Chem. Mater.*, 2005, **17**, 514.
6 J.-L. Pellegatta, C. Blandy, V. Colliere, R. Choukroun, B. Chaudret, P. Cheng and K. Philippot, *J. Mol. Catal. A: Chem.*, 2002, **178**, 55–61.
7 A. M. Trzeciak and J. J. Ziółkowski, *Appl. Organomet. Chem.*, 2004, **18**, 124.
8 V. Percec, J. G. Rudick, M. Peterca, M. Wagner, M. Obata, C. M. Mitchell, W.-D. Cho, V. S. K. Balagurusamy and P. A. Heinney, *J. Am. Chem. Soc.*, 2005, **127**, 15257.
9 S. Sakurai, K. Kuroyanagi, K. Morino, M. Kunitake and E. Yashima, *Macromolecules*, 2003, **36**, 9670.
10 R. Choukroun, D. de Caro, B. Chaudret, P. Lecante and E. Snoeck, *New J. Chem.*, 2001, **25**, 525.
11 C. I. Simionescu and V. Percec, *J. Polym. Sci., Polym. Chem. Ed.*, 1980, **18**, 147.
12 P. Mastrorilli, C. F. Nobile, A. Rizzuti, G. P. Suranna, D. Acierno and E. Amendola, *J. Mol. Catal. A: Chem.*, 2002, **178**, 35.

